Hydrogen scattering from a cesiated surface model

Maria Rutigliano[1], Amedeo Palma[2], Nico Sanna[3,1]

[1] CNR-NANOTEC (P.LAS.M.I. Lab), Via Amendola 122/D, 70126 Bari, Italy
[2] CNR-ISMN, Istituto per lo Studio dei Materiali Nanostrutturati, Via Salaria km 29.3, UOS Montelibretti, Monterotondo S. (RM), Italy
[3] CINECA, Via dei Tizii 6/b, 00185 Rome, Italy

Abstract

A cesiated surface model was considered to study the dynamics of hydrogen atom scattering using a semiclassical collisional method. Using dipole correction method, the work function of the considered surface, is calculated to be 1.81eV (± 0.02) eV. The Potential Energy Surface for the interaction of H atoms with the surface was determined *via* first principle electronic structure calculations including the interaction with both Cs and Mo atoms of the surface. We found the scattered H atoms to have a negative partial charge of nearly 0.4 with the backscattered flux arising mainly from H atoms impinging directly (or very close) to Cs atoms on the surface. On the contrary, H atoms impinging in the voids between the Cs atoms propagate through the first Cs layer and remain adsorbed. The propagation occurs mainly in the vertical direction. The scattering probability after a very quick increase remains almost constant around an average value of 0.35.

Keywords: Cesiated Surface; DFT calculations; Work function; Molecular Dynamics; Surface Processes;

1. Introduction

In the last years, the interest for the negative ion production increased significantly for its application in several fields spanning from microelectronics [1], [2] to magnetically confined fusion [3], from space propulsion [4] to injector for particles accelerators [5].

In low-pressure plasmas, two methods are commonly used for the production of negative hydrogen ions: volume production and surface production. Volume production occurs *via* dissociative attachment of electron on molecules while surface production occurs *via* direct electron transfer from a low-work function surface metal to the H/D atoms impinging on [6]. In the case of surface production, the conversion yield depends on the work function of the surface. Since many years it is well know that the high efficiency in the production of negative ions, results from the interaction of plasma particles with electrodes on which cesium has been adsorbed [7].

Electronic structure calculations were used in the past to study the properties of a clean Mo(001) surface and the bonding between a dense Cs overlayer with the same substrate [8]. In a recent paper [9] Density Functional Theory (DFT) calculations were used in conjunction with Coupled-Cluster (CC) method to give a very accurate description of an incomplete and irregular Cs layer on Mo surface, mimicking a more realistic surface.

In this work, the interaction of hydrogen atom with a cesiated surface model provided courteously by the group of Ref. [9], was studied. First, we determined the work function of considered surface model using dipole correction method [10]. Then the dynamics of interaction was investigated *via* Molecular Dynamics (MD) calculations using the semiclassical collisional method [11] capable to take into account the coupling of surface phonons during the interaction. As in any MD calculations the most critical issue is the achievement of a very accurate Potential Energy Surface (PES) where the reaction takes place. To this end, we performed DFT calculations for the interaction of H atom on the cesiated surface model. These calculations allow getting another important result of this work, i.e. the interaction potential for a hydrogen atom and the net charge transfer between the impinging species and the surface.

Then, we propagated thousands of trajectories to determine the probabilities of surface processes and obtain insights on the reaction mechanism and its dependence on the surface topology. The surface processes studied in MD calculations occurs on a time scale of fs, even if applicative process occurs on a longer time scale.

Therefore, this work aims to shed light on the interaction mechanism of hydrogen atoms with a cesiated surface at atomic level and determine accurate collisional data needed as input in Particle In Cell (PIC) self-consistent kinetic plasma models [12], used to describe on the real time scale the formation of negative ions.

The importance of this kind of calculations is to have a predictive character for the choice of the right surface for applicative purposes.

2. Computational Setup

2.1 Surface Model

The surface model consists of 604 atoms, 563 Mo atoms and 41 Cs atoms disposed on the first top layer (see Fig.1(a)). The density of Cs atom on the surface is of 1.65 x10^{15} atom.cm^{-2}. From this large crystal we cleaved a slab having a partial cesium layer on top of three molybdenum layers along the [001] direction, mimicking the situation of medium Cs coverage, given by a Mo (5x5) surface unit cell (A=B=18.74Å) containing 108 Mo and 10 Cs atoms (see Fig1(b)). The slab is subject to Periodic Boundary Conditions (PBC) and our supercell includes a vacuum region of 15 Å to avoid spurious interactions with its images.

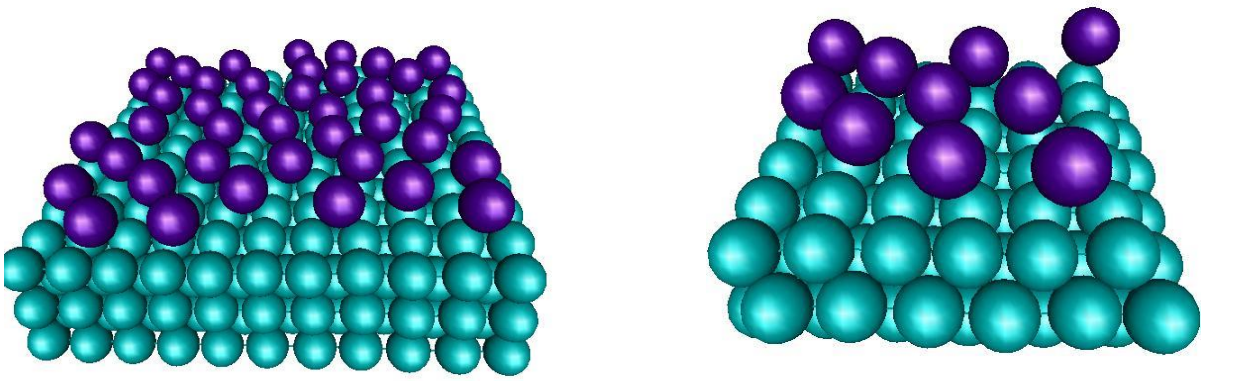

Fig.1: (a) 3D Cesiated Surface Model as determined in Ref. [9]; (b) Slab used in DFT calculations.

Slab calculations were performed with Quantum Espresso code [13] using the same functional of Ref. [9], by evaluating electronic structure within DFT using Perdew-Burke-Ernzerhof (PBE) functional for exchange and correlation energy [14] [15] and open shell system is treated within the unrestricted formalism. We adopt a plane-wave pseudopotentials (PP's) expansion [16] [17] using ultrasoft Vanderbilt PP's for H atoms [18], and Martins-Troullier PP [19] for Cs and Mo atoms. Both heavy atoms pseudopotentials were generated (see pseudopotentials library in Ref. [13]) by scalar relativistic calculations. We use energy cut-offs of 50 and 410 Rydberg to truncate the plane-waves

expansion of the pseudo wave functions and of the augmented charge density, respectively; the equations of motions were integrated with a time step of 10 a.u. (0.242 fs). The Brillouin zone was sampled by (2*2*1) Monkhorst and Pack points [20]. All DFT calculations are performed using PWSCF module [13] and, in case of optimization runs, forces are relaxed using Broyden–Fletcher–Goldfarb–Shanno (BFGS) algorithm.

Dipole correction [10] was also applied to determine the work function (ϕ) of the partially covered Cs surface since it has been calculated as a difference between the plane averaged electrostatic potential in the vacuum region and the Fermi level. For this calculation, we adopted a symmetric slab model where a Cs layer is placed both on top and below the Mo layers.

The interaction of Mo atoms with Cs surface atoms was described using our slab model in which the interaction potential was built by a multiple approach as in Ref. [9]. In that work the Mo-Cs interactions in gas phase were evaluated by accurate *ab initio* calculations while DFT calculations were performed for the Cs adsorption on Mo [001] surface.

2.2 The Potential Energy Surface

To evaluate the interaction potential between an impinging H atom with the Cs atoms on the surface we have performed scans for different heights of H atom approaching perpendicularly on top of each Cs atoms. The interaction potential was obtained by subtracting from the energy of the system slab+H (E_{slab+H}) the energy of isolated non-interacting H atom (E_H) and of isolated slab (E_{slab}). We chose this direction of interaction because along the perpendicular approach the surface has its maximum exposition to the impinging flux.

In Figure 2(b) the interaction potential as a function of distance from the surface for each Cs atom on the slab, as obtained from ab initio calculations, is shown. It appears that the interaction potential for H atom impinging on the different Cs atoms is very similar, except for Cs_112, for which we found its minimum value (~ -0.97eV) and Cs_110 for which we found its maximum (~ -0.53eV). The minimum distance of interaction for the complete set of curves is placed at 2.8Å. Then we proceeded to a sampling of the sites on the surface, by introducing a sort of coordination number (CN) defined as the number of Cs atoms for which the distance is in the range [4-5]Å, corresponding to the minimum of potential Cs-Cs reported in Ref. [9], for a given Cs atom. The *ab initio* reference interaction potential model considered in the building up of PES according to the CN number described so far, is reported in Table 1.

Table 1. *Ab initio* interaction potential considered in the PES building up according to the CN value and corresponding parameters used in Eq. (1).

CN value	reference potential	D_α(eV)	β_α(Å^{-1})	re_α(Å)
0	Cs_110	0.24	1.20	3.88
1	Cs_113	0.58	1.00	3.60
2	Cs_118	0.46	1.00	3.58
3	Cs_114	0.45	1.00	3.68
4	Cs_112	0.45	0.95	3.60

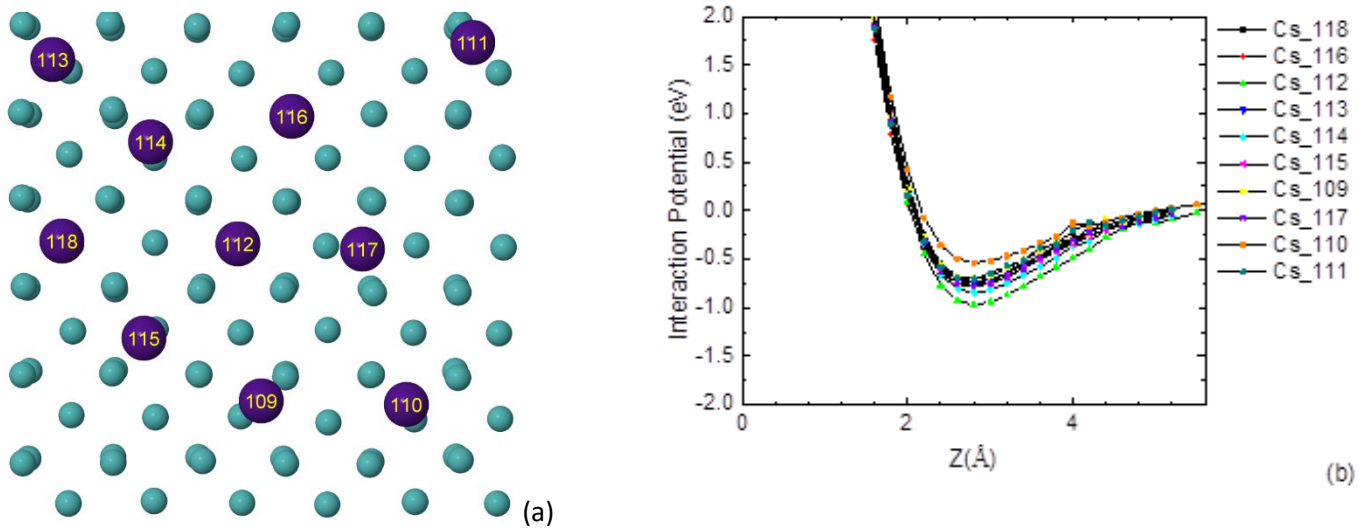

Fig.2: (a) Top view of slab used in the calculation, labels refer to Cs atoms considered in the calculations; (b) Interaction potential for H atom impinging on surface Cs atoms.

Due to the fact that between the Cs atoms on the first top layer there are large voids, the impinging H atom can undergo also the interaction of Mo atoms placed on the first layer below the Cs layer, placed at nearly -3 Å (assuming the Cs layer as our reference at Z=0). For this reason, we carefully analysed the topology of the surface and the relative positions of Cs atoms with respect to underlying Mo atoms, thus identifying four characteristics positions given by the Mo atoms labelled in Fig. 3a. Then

we calculated the interaction potential for H atom impinging directly on these Mo atoms; Fig. 3b reported the final H-Mo interaction potential obtained by DFT calculations.

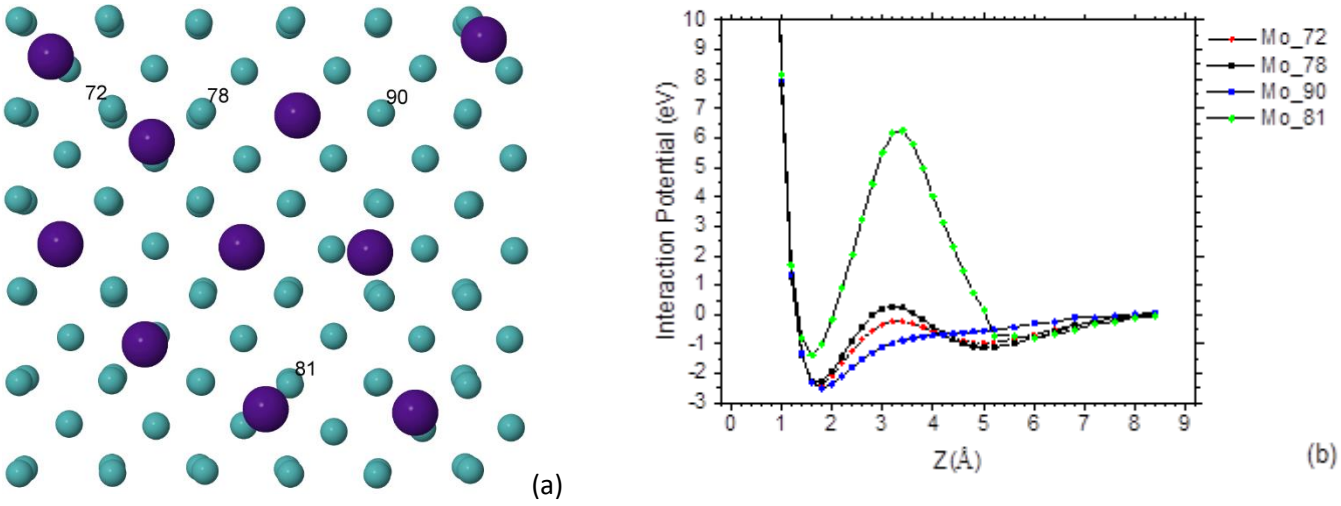

Fig.3: (a) Top view of slab used in the calculation, Mo atoms used in the calculations are labelled; (b) Interaction potential for a H atom impinging on different Mo surface atoms.

In Fig. 3(b) it is significant the presence of a barrier placed at nearly z = 3Å, distance corresponding to the first layer of Cs atoms. The barrier decreases going from atom Mo_81 to atom Mo_90 for which the barrier completely disappears. This circumstance can be ascribed to the fact that Mo_90 is not very close to the surrounding Cs atoms.

In DFT calculations, for each kind of H interaction we determine from 24 to 32 points along Z.

To make these data usable in the semiclassical collisional method [11] it is necessary to post-fit them in order to obtain curves given as sum on pair-interactions between the impinging H atom and the atoms in the crystal. For the interaction of H with Cs atoms the functional shape for the potential is described as:

$$V_{H-Cs} = \sum_{i=1}^{N_{Cs}} D_\alpha * e^{-\beta_\alpha * (R_i - re_\alpha)} * \left(e^{-\beta_\alpha * (R_i - re_\alpha)} - 2\right) \quad (1)$$

where N_{Cs} is the total number of Cs atoms in the lattice used in the dynamics calculations and reported in Fig.1(a), and the α ranges between 0 and 4 according the values of CN for the considered Cs. The parameters D_α, β_α and re_α are those reported in Table 1.

The functional form of the interaction potential of H on the selected Mo atoms depends on the considered Mo atom and on its distance from the surface. Basically, the potential is fitted by combining Morse-like function with exponential or sine function. The detailed expression for the interaction potential of H atom on Mo atoms is reported in Appendix 1.

Finally, the complete PES for the interaction of H atom on the cesiated surface is given by:

$$V(r_i, r_j) = \sum_{i=1}^{N_{Cs}} V_{H-Cs}(r_i) + \sum_{j=1}^{N_{Mo}} V_{H-Mo}(r_j) \quad (2)$$

where $V_{H\text{-}Cs}$ is given in Eq. (1) and $V_{H\text{-}Mo}$ is given by the expressions reported in Appendix 1.

In Figure 4(a)-(b) two planar projection of the potential for Z=2.5Å and Z=6.0Å are reported.

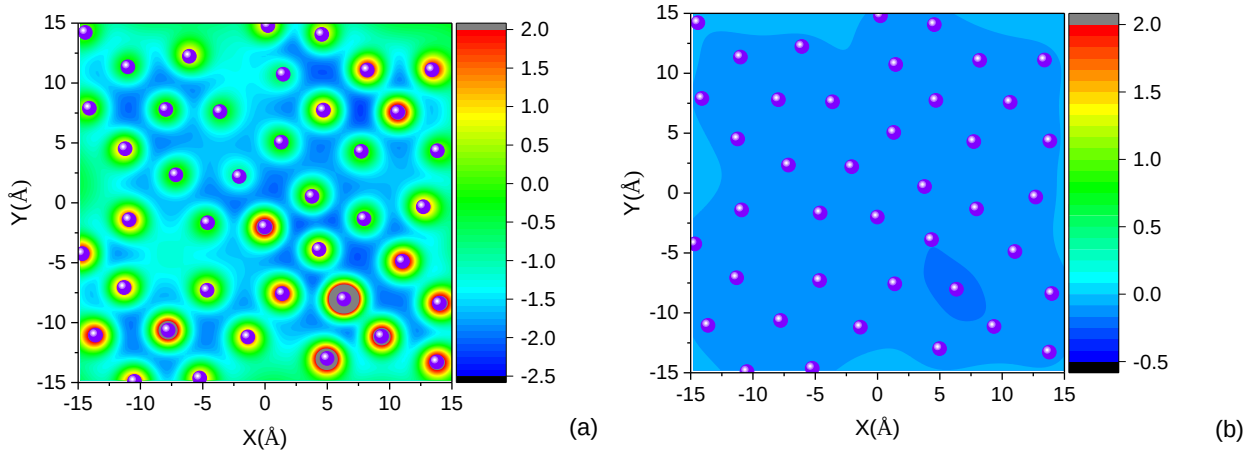

Fig.4: X-Y projection of the PES for (a) Z=2.5Å and (b) Z=6Å. Violet dots indicate the positions of Cs atoms on the surface

DFT calculations enabled also to calculate the charge transfer from the impinging atom and the atom on the surface. Atomic partial charges are evaluated by Loewdin population analysis by projecting plane wave eigenfunctions into atomic orbitals as implemented in Ref. [13]. From this analysis, we can deduce that a local interaction occurs between the gas-phase H atom and the considered Cs atom. The charge transferred to the H atom is reported in Fig.5 for Cs atoms, considered in the building up of PES, (Fig. 5a) and Mo atoms (Fig.5b) as a function of the distance from the surface.

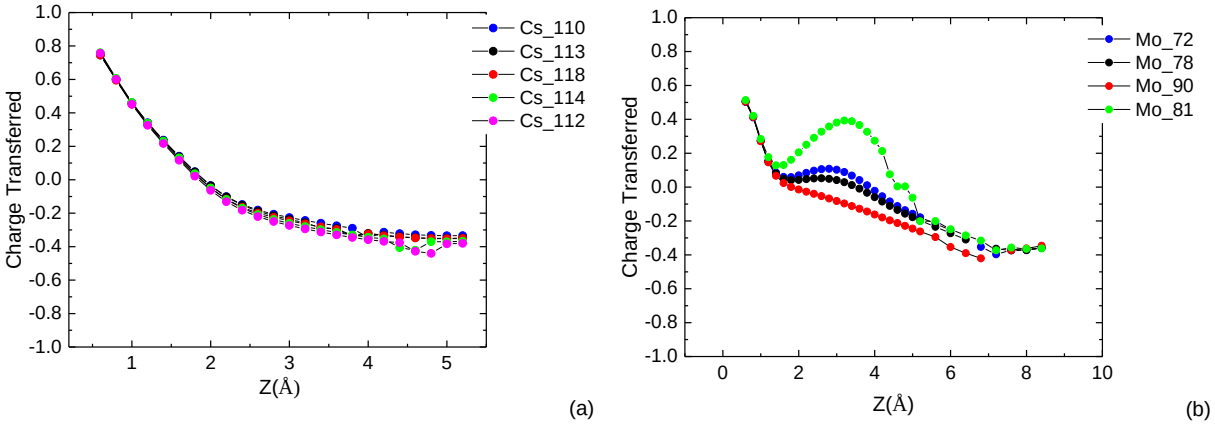

Fig.5: Charge transfer during the interaction to the gas-phase H atom with Cs (a) and Mo atoms (b) as evaluated by *ab initio* calculations.

Therefore, looking at Fig. 5, we can say that the mean field potential determined and used in the study of scattering dynamics, takes into account the fact that the H atom is backscattered in gas-phase with a partial charge of 0.4, mainly due to the repulsive interaction with the first layer Cs atoms.

2.3 Semiclassical Collisional Method

The interaction of H atoms impinging on the cesiated surface model in Fig.1 was studied using the semiclassical collisional method [11]. The method was used successfully to describe the interaction of atom and molecules with metallic and non-metallic surfaces (see for example Refs. [21]-[23]). The calculations proceed *via* the solutions of phonon dynamics of the considered surface model, then the determination of interaction potential between the impinging species and the substrate and finally the integration of trajectory. The method is semiclassical in the sense that the gas-phase species are treated classically by solving the Newton motion equations, while the phonons of the solid are treated quantum mechanically by solving the time-dependent Schrödinger equations of motion under the harmonic oscillator approximation. In other words, we are assuming that a set of M = 3N - 6 (N is the number of atoms in the 3D lattice) independent harmonic oscillators are perturbed by a linear force exerted between the atom approaching the surface from the gas-phase and the solid substrate. Then the motion of H atom is obtained by solving the motion equation in the presence of an effective Hamiltonian, H_{eff}:

$$\dot{r} = \frac{p_r}{m} \qquad \dot{p_r} = -\frac{\partial H_{eff}}{\partial r} \tag{3}$$

where r and p_r are the distance and the momentum of impinging atom, respectively; $\dot{r}$ and $\dot{p_r}$ are the derivative respect to time and H_{eff} is the expectation value on the phonon wavefunction of interaction potential between the gas-phase atom and the surface:

$$H_{eff} = V_0 + V_{add}(t, T_S) \tag{4}$$

with V_0 the static interaction potential and V_{add} the dynamical Hamiltonian, function of the interaction time t, the surface temperature T_S, and the excitation/de-excitation processes of the phonon modes.
We have determined the phonon dynamics by using the potential derived in [9] for the interaction Cs-Cs, Mo-Mo and Mo-Cs in the lattice. Due to the non- crystalline structure of lattice, we obtain a spectra characterized by a broad band for large frequencies and sparse spikes at lower frequencies 0.5 and 1.0THz attributable to the Cs atoms on the first layer [24]. The PES assumed in the calculations is that determined in the previous section and given by Eq. (2).
The H atom impinges normally to the surface from a distance of 8Å with planar coordinates chosen randomly in an aiming area of 15Å x 15Å. The kinetic energy of atom is changed in the range [0.3-5.0] eV and the surface temperature is fixed at 1000K. For each collisional energy a bunch of 4000 trajectories have been propagated, a number large enough to assure the convergence of the obtained surface process probabilities within 10%, the error percentage of which suffers the method. The integration step was of 0.05 fs and the accuracy required in the integration procedure was of 10^{-5}. The integration of equation of motion was done *via* the Hamming modified Predictor Corrector method including fourth order Runge-Kutta method for adjustment of the initial increment and for computation of initial values.

3. Results and Discussion

In Figure 6 a graphical representation of the work function (ϕ) calculation is given. Here we evaluate ϕ from the difference between averaged electrostatic potential in the vacuum and the Fermi level. This computation was performed on a symmetric slab with Cs atoms on both surface layers (i.e. on top and below Mo layers) and we obtain a value of 1.81 eV. This result is in line with the experimental and theoretical investigation on the role played by Cs atoms in increasing the performance of negative

ion sources [3], [7], [25], [26]. It is worth to remind that the work function for pure Mo and Cs metals is 4.36 and 1.95 eV respectively [27]. A work function value of 1.61 eV was obtained from experimental visible and X-ray photoelectron spectroscopy of an Au(111) surface at a well-defined sub-monolayer coverage of cesium in [28].

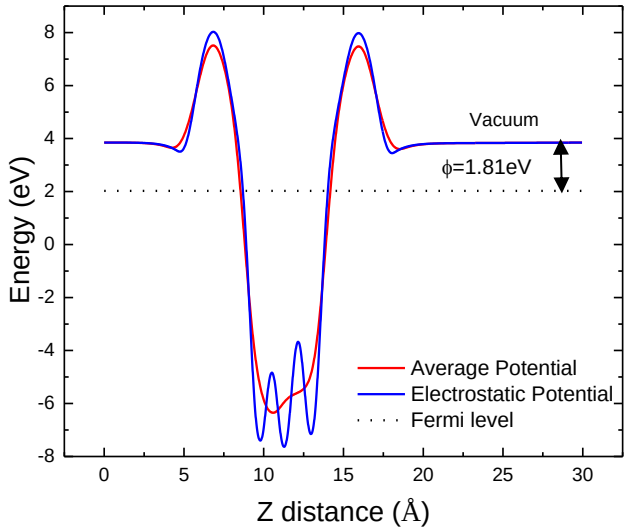

Fig. 6: Average electrostatic potential along the z-axis perpendicular to the surface in the cell subject to Periodic Boundary Conditions. Difference between electrostatic potential in the vacuum and Fermi level gives the work function (ϕ) value of 1.81 eV.

Using the previously described PES in our semiclassical collisional dynamics method, we determine the recombination for the two possible and competitive surface processes: scattering and adsorption. By defining the energy available to escape from adsorption well as $V_{esc}= E_{tot}- \Delta E_{ph}$, being E_{tot} the trajectory total energy and ΔE_{ph} the energy exchanged with the surface phonons, we assume that H is adsorbed when V_{esc} is less than V_{add} value (see Eq. (4)) at a specific interaction time. Following a second criterion one can say that H is adsorbed whenever the z component of the atom reaches the adsorption distance, $z_{ad} \sim 2.8$ Å, and the component of the momentum along the z direction is negative for at least few picoseconds. On the contrary, H atom is considered scattered in gas-phase when its distance from the surface is larger than 8 Å, where the interaction with the surface is negligible.

The probabilities for these processes as a function of kinetic energy of H atom are reported in Fig. 7(a). It appears that the scattering probability rises very fast at a nearly constant mean value of 0.35. Instead the adsorption probability decreases from the maximum value (~0.91) to a nearly constant

mean value of 0.65. From the scattering trajectories analysis, it appears that the reaction follows a direct mechanism and that the impinging atom is immediately backscattered in the gas-phase approximatively in the same direction as that of incidence. This can be easily seen looking at Fig.7(b) where the angular distribution for three different kinetic energies is reported. For the lowest collisional energy, the angular distribution is peaked at 5°, increasing the energy the peak of angular distribution approaches 0°.

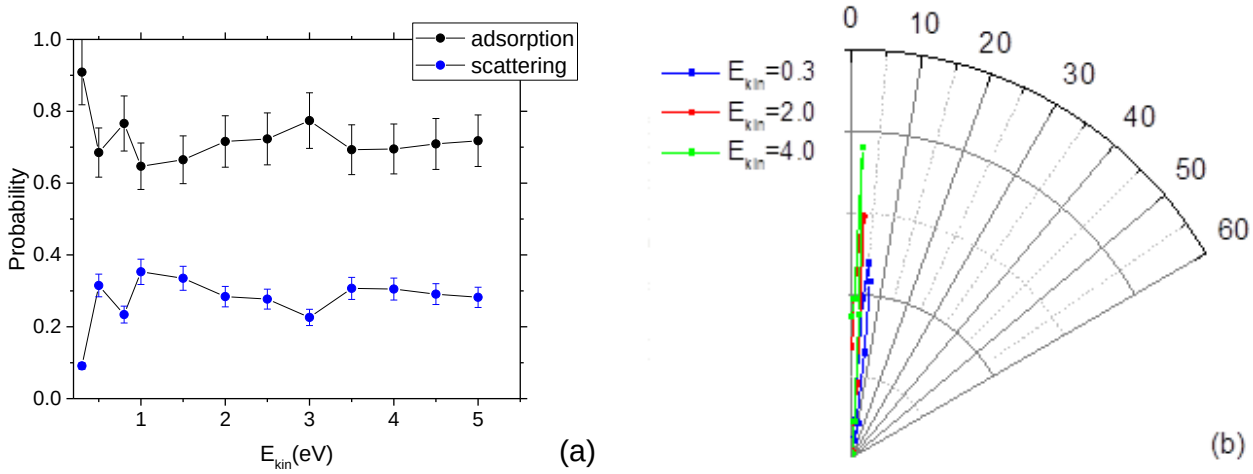

Fig.7: (a) Probability for H scattering and adsorption on the cesiated surface as a function of kinetic energy; (b) Angular distribution for H backscattered in gas-phase

We have also investigated the influence of initial impinging site on the trajectory fate. So we chose a bunch of 2000 trajectories and we projected on the surface the hydrogen initial planar coordinates for trajectories ending with a backscattering or adsorption event. We report the results of this study for E_{kin}=4.0eV in Fig.8(a-b). Looking at Fig. 8 (a) we can point out that in the majority of trajectories H atom is backscattered when impinges on top of a surface Cs atom. On the contrary, when H atom impinges on the voids between Cs atoms it is adsorbed, being attracted by underlying Mo atoms (see Fig. 8(b)). Unfortunately, trajectories can be followed just for few fs because of the instability in the trajectory as the value of z becomes negative. The instability of trajectories for negative z-values depends on the strong coupling with the bulk phonons. In spite of the fact that this well-known aspect introduces some limitations to the feasibility of MD approaches for investigating bulk processes, MD methods remain a well suited tool to studying surface desorption and surface reactions.

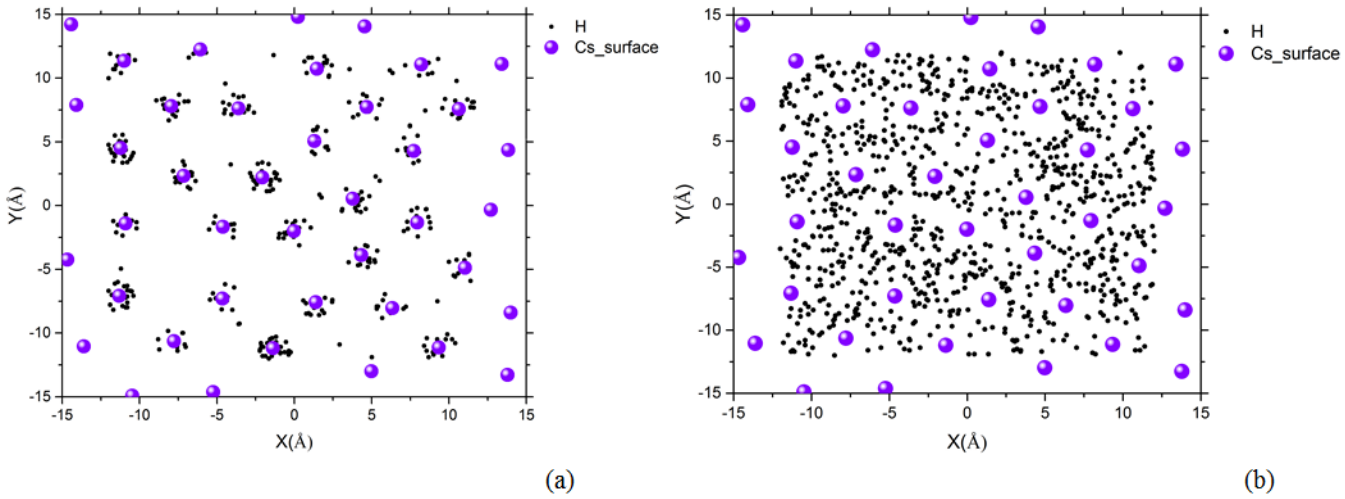

Fig.8: (a) X-Y planar position for H atom trajectories ended with backscattering; (b) the same as (a) but for trajectories ended with adsorption.

The dynamics for the two reaction channels is well defined since time evolution of each trajectory is overall very similar. A typical adsorption trajectory is reported in Fig.9(a)-(d) for E_{kin}=2.0eV. The H atom is accelerated toward the surface and when reaches the minimum interaction distance (at t~25fs) (see Fig.9(a)) its kinetic energy reaches the maximum. Then kinetic energy decreases and increases the interaction with the surface (V_{add}) and the atom remains adsorbed (see Fig. 9(c)). This suggests that a coupling exists between the translational motion of impinging H atom and the substrate phonons. It is also evident, from Fig. 9, that the motion in the plane, at least until we can follow the trajectory, is limited to a few tens of Å (see Fig. 9(b)).

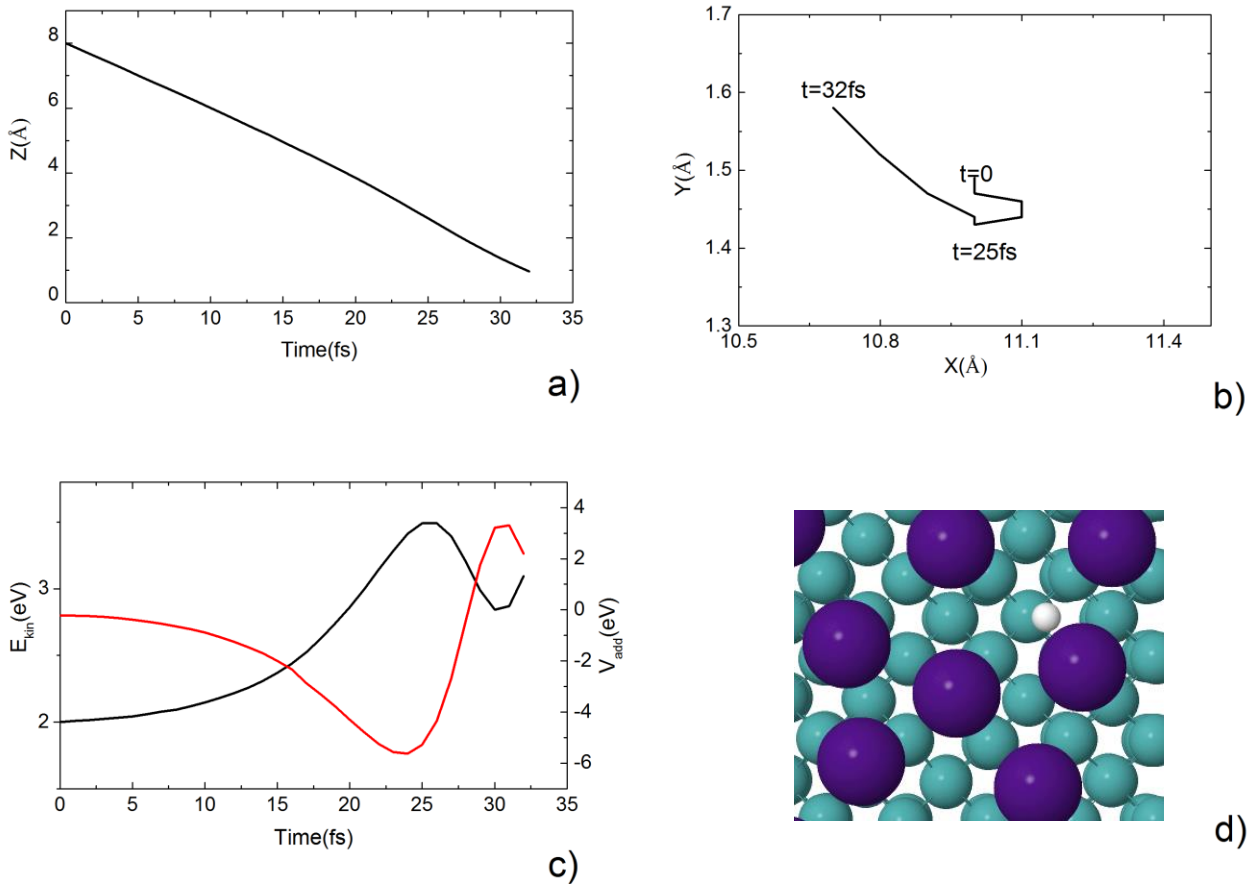

Fig.9: A typical adsorption trajectory of H atom on cesiated surface model (a) Z -coordinate as a function of collisional time. (b) X-Y coordinates as a function of time. (c) Kinetic energy as a function of time (black line left-end axis) and interaction energy (V_{add}) with the surface (red line). (d) Position of H atom (white ball) on the surface.

It is worth noting that the used collisional method enables us to determine, for each trajectory step, the energy exchanged between the impinging species and the substrate.

Then looking at this quantity it appears that for the complete range of considered collisional energy, the energy exchanged with the surface at the end of trajectory is extremely low (a few dozen Kelvin), and it is transferred from the surface to H atom. This can be ascribed to the fact that the system under study is characterized by a high mismatch both between the masses of interacting species and between the characteristic phonon frequencies. In particular, the H-surface stretching frequency of nearly 1500 THz, corresponding to the H adsorption energy, is much higher than cesium typical phonon frequency: as a result of such decoupled interaction the surface does not undergo any thermal damage.

Conclusions

The work function of a partially Cs covered Mo surface was determined together with a very accurate interaction potential for hydrogen atom interacting with the same surface model. The calculated work function value of 1.81 eV is in agreement with what expected from experimental evidences, confirming that Cs covered surfaces could be an interesting source of negative ions for fast neutral beam generation employed in nuclear fusion.

The obtained PES was used to simulate the interaction dynamics for a flux of hydrogen impinging on the surface.

We found that Cs atoms on the surface promote the reflection of impinging H atoms *via* a direct mechanism in a direction close to the specular one. Such atoms are characterized by a partial negative charge. On the contrary, when atoms impinge on the voids between Cs atoms (hollow sites) the gas-phase atom remains adsorbed on the surface.

The next goals of this research project will be the investigation of H isotopes (such as deuterium) interaction with the surface and the study of H_2 molecule formation on the cesiated surface model to clarify how presence of roto-vibrationally excited hydrogen molecules can influence the properties of plasma bulk.

Acknowledgements

The authors are grateful to Prof. S. Longo (University of Bari) for providing the model surface, and to Prof. V. Fiorentini (University of Cagliari, I) for fruitful discussions on work function evaluation. We would like also to thank CINECA for computational facilities in the framework of ISCRA calls under the project IsC42_HyonMoCs and Computing resources provided by CRESCO/ENEAGRID High Performance Computing infrastructure and its staff (see http://www.cresco.enea.it for information).

References

[1] C. Thomas, Y. Tamura, T. Okada, A. Higo and S. Samukawa, Estimation of activation energy and surface reaction mechanism of chlorine, J. Phys.D: Appl. Phys. **47** (2014) 275201.

[2] C. Thomas, Y. Tamura, M. E. Syazwan, A. Higo and S. Samukawa, Oxidation states of GaAs surface and their effects on neutral beam etching, J. Phys. D: Appl. Phys. **47** (2014) 215203.

[3] U. Fantz, P. Franzen and D. Wunderlich, Development of negative hydrogen ion sources for fusion: Experiments and modeling, Chem. Phys. **398** (2012) 7–16,.

[4] S. Mazouffre, Electric propulsion for satellites and spacecraft: established technologies and novel approaches, Plasma Sources Sci. Technol. **25** (2016) 033002.

[5] A. Ueno, H. Oguri, K. Ikegami, Y. Namekawa and K. Ohkoshi, Interesting experimental results in Japan Proton Accelerator Research Complex H^- ion-source development, Rev. Sci. Instrum. **81** (2010) 02A720.

[6] M. Bacal and M. Wada, "Negative hydrogen ion production mechanisms, Appl. Phys. Rev. **2** (2015) 021305.

[7] V. Dudnikov, Thirty years of surface plasma sources for efficient negative ion, Rev. Sci. Instrum. **73**, p. (2002) 992.

[8] S. R. Chubb, E. Wimmer, A. J. Freeman, J. R. Hiskes and A. M. Karo, All-electron local-density-functional theory of alkali-metal adsorption on transition-metal surfaces: Cs on Mo(001), Phys. Rev. B **36**(1987) 4112-4122.

[9] A. Damone , A. Panarese, C. M. Coppola, J. Jansky, C. Coletti, L. Chiodo, G. Serianni, V. Antoni and S. Longo, Theoretical determination of the microstructure of Cs covering of Mo in negative ion sources for nuclear fusion applications, Plasma Phys. Control. Fusion, **57** (2015) 035005.

[10] L. Bengtsson , Dipole correction for surface supercell calculations, Phys. Rev. B **59** (1999) 12301-12304.

[11] G. D. Billing, Dynamics of Molecule Surface Interactions, JohnWiley & Sons, New-York, 2000.

[12] F. Taccogna and P. Minelli, PIC modeling of negative ion sources for fusion, New Journal of Physics, **19** (2017) 015012.

[13] P. Giannozzi, S. Baroni, N. Bonini, M. Calandra, R. Car, C. Cavazzoni, D. Ceresoli, G. L. Chiarotti, M. Cococcioni, I. Dabo, A. Dal Corso, S. Fabris, G. Fratesi, S. de Gironcoli, R. Gebauer, U. Gerstmann, C. Gougoussis, A. Kokalj, M. Lazzeri, L. Martin-Samos, N. Marzari, F. Mauri, R. Mazzarello, S. Paolini, A. Pasquarello, L. Paulatto, C. Sbraccia, S. Scandolo, G. Sclauzero, A. P. Seitsonen, A. Smogunov, P. Umari, R. M. Wentzcovitch, QUANTUM

ESPRESSO: a modular and open-source software project for quantum simulations of materials, J. Phys.: Condens. Matter 21(2009) 395502.

[14] J. P. Perdww, K. Burke and M. Ernzerhof, Generalized Gradient Approximation Made Simple, Phys. Rev. Lett. 77 (1996) 3865-3868.

[15] J. P. Perdew, K. Burke and M. Ernzerhof , Erratum of Generalized Gradient Approximation Made Simple, Phys. Rev. Lett. 78 (1997) 1396, 1997.

[16] A. Pasquarello, K. Laasonen, R. Car, C. Lee and D. Vanderbilt, Ab initio molecular dynamics for d-electron systems: Liquid copper at 1500 K,Phys. Rev. Lett. 69 (1992) 1982-1985.

[17] K. Laasonen, A. Pasquarello, R. Car, C. Lee and D. Vanderbilt, Car-Parrinello molecular dynamics with Vanderbilt ultrasoft pseudopotentials, Phys. Rev. B 47 (1993) 10142-10153.

[18] D. Vanderbilt, Soft self-consistent pseudopotentials in a generalized eigenvalue formalism, Phys. Rev. B 41 (1990)7892-7895.

[19] J. L. Martins and N. Troullier , Structural and electronic properties of KnC60, Phys, Rev. B 46 (1992) 1766-1772.

[20] H. J. Monkhorst and J. D. Pack, Phys. Rev. B **13** (1976) 5188.

[21] M. Cacciatore and G. D. Billing, Dynamical relaxation of H_2(v,j) on a copper surface, Surf. Sci. **232** (1990) 35.

[22] M. Rutigliano, M. Cacciatore and G. D. Billing, Hydrogen atom recombination on graphite at 10K via the Eley-Rideal mechanism, Chem. Phys. Lett. **340** (2001) 13-20.

[23] C. Zazza, M. Rutigliano, N. Sanna, V. Barone and M. Cacciatore, Oxygen Adsorption on β-Quartz Model Surfaces: Some Insights from Density Functional Theory Calculations and Semiclassical Time-Dependent Dynamics, J. Phys. Chem. A **116** (2012) 1975−1983.

[24] J. Xie, S. P. Chen, J. S. Tse, D. D. Klug, Z. Li, K. Uehara and L. G. Wang, Phonon instabilities in high-pressure bcc-fcc and the isostructural fcc-fcc phase transitions of Cs, Phys. Rev. B **62** (2000) 3624-3629.

[25] P. Diomede and S. Longo, Monte Carlo Cs^+ transport from a point source in negative ion sources: effect of the deuterium flow, Plasma Sources Sci. Technol. **19** (2009) 015019.

[26] P. Diomede and S. Longo, Momentum transfer Cs^+/H_2 cross section from an inversion of transport data, The European Physical Journal D **67** (2013) 1-4.

[27] J. Speight, Lange's Handbook of Chemistry 16th ed., McGraw-Hill Professional, Boston, MA, 2004.

[28] J. L. LaRue, J. D. White, N. H. Nahler, Z. Liu, Y. Sun, P. A. Pianetta, D. J. Auerbach and A. M. Wodtke, The work function of submonolayer cesium-covered gold: A photoelectron spectroscopy study, J. Chem. Phys. **129** (2008) 024709.

[29] R. D. Diehl and R. McGrath, Current progress in understanding alkali metal adsorption on metal surfaces, J. Phys. Condens. Matter **9** (1997) 951-968.

Appendix 1

Functional expression for the interaction potential of H atom on sampled Mo surface atoms (label are that given in Fig.3 (a):

Mo_78:

$$V_{H-Mo} = \sum_{i=1}^{N_{Mo}} D_{A1} * e^{-\beta_{A1}*(R_i - re_{A1})} * \left(e^{-\beta_{A1}*(R_i - re_{A1})} - 2\right) \qquad z < 2.4\text{Å} \quad \text{(A1)}$$

$$V_{H-Mo} = \sum_{i=1}^{N_{Mo}} (-0.0208 * sin(\pi * (R_i - re_{A2}))) - 0.0013 \qquad 2.4\text{Å} \leq z \geq 4.0\text{Å} \quad \text{(A2)}$$

$$V_{H-Mo} = \sum_{i=1}^{N_{Mo}} D_{A2} * e^{-\beta_{A2}*(R_i - re_{A2})} * \left(e^{-\beta_{A2}*(R_i - re_{A2})} - 2\right) + 0.00025 \qquad z > 4.0\text{Å} \quad \text{(A3)}$$

Mo_72

$$V_{H-Mo} = \sum_{i=1}^{N_{Mo}} D_{B1} * e^{-\beta_{B1}*(R_i - re_{B1})} * \left(e^{-\beta_{B1}*(R_i - re_{B1})} - 2\right) \qquad z < 2.4\text{Å} \quad \text{(A5)}$$

$$V_{H-Mo} = \sum_{i=1}^{N_{Mo}} (-0.0308 * sin(\pi * (R_i - re_{B2}))) - 0.0013 \qquad 2.4\text{Å} \leq z < 3.85\text{Å} \quad \text{(A6)}$$

$$V_{H-Mo} = \sum_{i=1}^{N_{Mo}} D_{B2} * e^{-\beta_{B2}*(R_i - re_{B2})} * \left(e^{-\beta_{B2}*(R_i - re_{B2})} - 2\right) + 0.00064 \qquad z \geq 3.85\text{Å} \quad \text{(A7)}$$

Mo_90

$$V_{H-Mo} = \sum_{i=1}^{N_{Mo}} D_{C1} * e^{-\beta_{C1}*(R_i - re_{C1})} * \left(e^{-\beta_{C1}*(R_i - re_{C1})} - 2\right) \qquad z \leq 2.0\text{Å} \quad \text{(A8)}$$

$$V_{H-Mo} = \sum_{i=1}^{N_{Mo}} D_{C2} * e^{-\beta_{C2}*(R_i - re_{C2})} \qquad z > 2.0\,\text{Å} \quad \text{(A9)}$$

Mo_81

$$V_{H-Mo} = \sum_{i=1}^{N_{Mo}} D_{D1} * e^{-\beta_{D1}*(R_i - re_{D1})} * \left(e^{-\beta_{D1}*(R_i - re_{D1})} - 2\right) \qquad z < 1.98\text{Å} \quad \text{(A10)}$$

$$V_{H-Mo} = \sum_{i=1}^{N_{Mo}} D_{D2} * e^{-\beta_{D2}*(R_i - re_{D2})} * \left(e^{-\beta_{D2}*(R_i - re_{D2})} - 2\right) \qquad 1.98\text{Å} \leq z \leq 3.8\text{Å} \quad \text{(A11)}$$

$$V_{H-Mo} = \sum_{i=1}^{N_{Mo}} D_{D3} * e^{-\beta_{D3}*(R_i - re_{D3})} * \left(e^{-\beta_{D3}*(R_i - re_{D3})} - 2\right) + 0.00025 \qquad z > 3.8\text{Å} \quad \text{(A12)}$$

where N_{Mo} is the total number of Mo atoms in the lattice used in the dynamics calculations and the parameters are reported in Table A.

Table A: Parameters for interaction potential of impinging H atom with Mo atom in the lattice

Label (i)	D_i(eV)	β_i($Å^{-1}$)	re_i(Å)
A1	0.565	1.75	5.78
A2	0.027	0.58	10.21
B1	0.55	1.75	5.78
B2	0.038	0.53	10.38
C1	0.52	1.60	6.00
C2	2.15	1.1	4.6
D1	0.315	2.10	5.83
D2	0.105	0.57	9.20
D3	0.020	0.71	11.15